Mitigation of Critical Current Degradation in Mechanically Loaded Nb_3Sn Superconducting Multi-Strand Cables by Ice Molding

Kazutaka SEO, Arata NISHIMURA, Yoshimitsu HISHINUMA, Kazuya NAKAMURA[1)], Tomoaki TAKAO[1)], Gen NISHIJIMA[2)] and Kazuo WATANABE[2)]

National Institute for Fusion Science, Oroshi-cho 322-6, Toki-city, Gifu 509-5292, Japan
[1)]*Sophia University, 7-1 Kioicho, Chiyoda-ku, Tokyo 102-8554, Japan*
[2)]*IMR, Tohoku University, Katahira 2-1-1, Aoba-ku, Sendai, Miyagi 980-8577, Japan*

(Received 28 August 2007 / Accepted 18 April 2008)

We have developed a novel critical current and stability measurement experimental setup, which utilizes a closed electric circuit with a multi-strand superconducting cable. The feature of this setup is mechanical loading applied to the multi-strand cable in the transverse direction. It was reported that Lorentz forces caused degradation in the critical current of the ITER-TFMC conductor. Furthermore, these phenomena were mainly observed in the ITER full-size conductors with large Lorentz forces under high magnetic fields. The advantage of our setup is critical current measurement under mechanical stresses comparable to those in the full-size conductor under high magnetic fields. By employing an inductive critical current measurement technique, we conducted an experiment with a transport current of about 10 kA without any power supply or current leads. In our experiments, we observed significant degradation in critical currents due to a compressive stress of about 30 MPa. We applied an innovative technique to mitigate the critical current degradation in mechanically loaded Nb_3Sn superconducting multi-strand cables. We molded one such cable with ice and tested it. No degradation occurred in the ice-molded cable. In addition, stability was also ensured due to the large thermal conductivity of ice. Thus, we have successfully mitigated the degradation in the critical current of the Nb_3Sn conductor by ice molding.

© *2008 The Japan Society of Plasma Science and Nuclear Fusion Research*

Keywords: Nb_3Sn, critical current degradation, transverse load, cable-in-conduit conductor, ice molding

DOI: 10.1585/pfr.3.042

1. Introduction

In a fusion device magnet, where magnetic fields and electromagnetic forces are large, large amounts of structural materials are necessary. In particular, the inboard radial build of tokamaks is tight, even though the stress in this inboard region is high. Therefore, in this region, the volume fraction of structural material is increased and that of the superconductor is decreased. This results in a high current density in the superconductor. Volume fractions of constituting components are described in Fig. 1 [1, 2]. The graphs represent the fractions of individual components at the inboard sections of the TF coils in ITER [1]. Structural materials—coil cases, radial plates, and conduits—are dominant. All component materials have their own roles, and this combination is designed through optimization. For extending this design to a future fusion reactor with size comparable to ITER, the amount of structural components will increase and that of the superconductor will decrease compared to that in ITER. Hence, this is the biggest conflict in coil design.

Superconductors with critical current densities under both high magnetic fields and large mechanical stresses will be required in future. Transverse stress effects have been reported for the ITER superconducting model coils [3]. For instance, in the ITER toroidal field (TF)

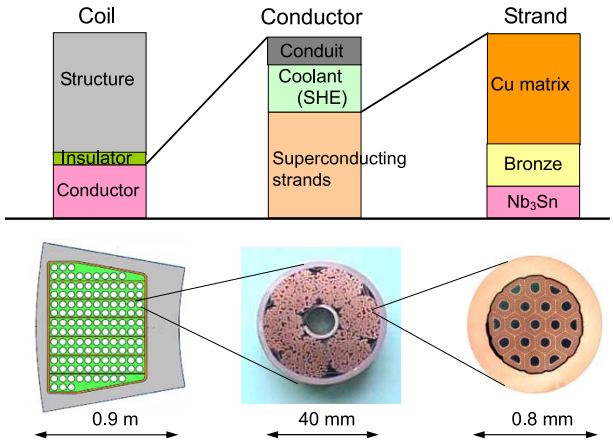

Fig. 1 Volume fractions of components comprising the inboard portion of the ITER TF coils [1, 2].

author's e-mail: seo@nifs.ac.jp

© 2008 The Japan Society of Plasma Science and Nuclear Fusion Research

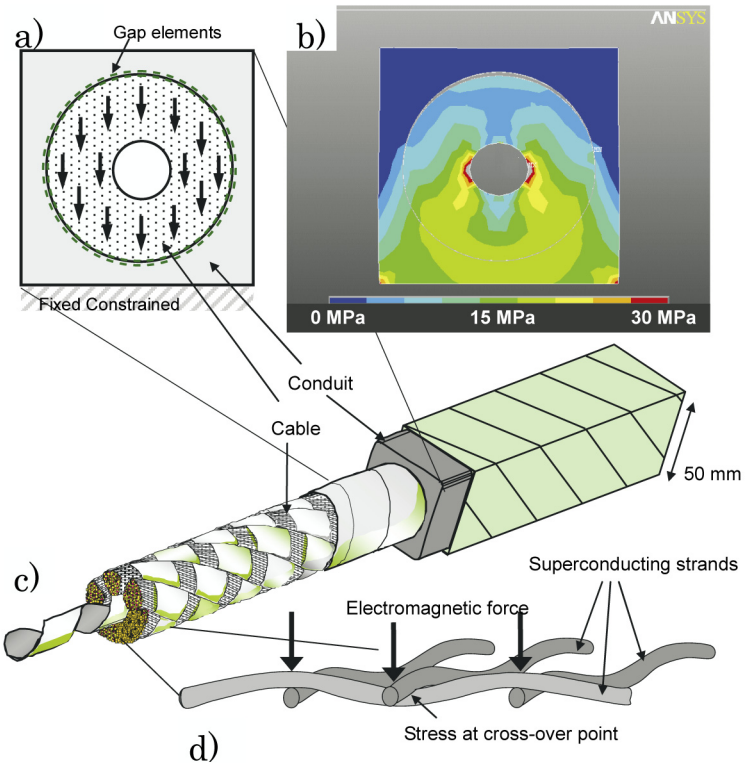

Fig. 2 Schematic illustration of the mechanism of degradation. a) The mechanical simulation model, b) distribution of von Mises stress, c) schematic illustrations of CICC, and d) local deformations of superconducting strands [2].

model coil (TFMC), the effective strain was reported to be about −0.8% based on Summers' scaling law, which corresponds to a critical current less than 1/3 of the zero strain critical current [4].

This phenomenon is described in Fig. 2. In Fig. 2 a), the finite element method (FEM) model simulating a cable in the conduit conductor (CICC) is presented. The Lorentz force is a body force in the cross section of the cable. Gap elements are employed between the conduit and cable. In Fig. 2 b), the von Mises stress distribution in the cross section of the conductor is shown for a net electromagnetic force of 800 kN/m. Since a large transverse electromagnetic force stress, such as 20 MPa, is applied to the strands, they are periodically bent or pinched, as shown in Fig. 2 d). On the other hand, superconducting materials for high magnetic field application, i.e., A15 and high critical temperature (T_c) superconductor (HTS), are mechanically brittle. Degradation due to large electromagnetic forces will therefore be a critical issue in the next generation fusion reactors, in which larger electromagnetic forces will be applied to the conductors.

The requirements to mitigate this degradation have drastically increased. We have set up a simple experiment to investigate the degradation due to transverse loading under high magnetic fields [5, 6]. We named our experimental project TRAnsversally Pressed Superconducting cable loop Experiment, TRAPSE. Our test was based on electromagnetic induction by a bias superconducting magnet [7, 8], whose nominal field was 18 T. By using the induction current, the test procedure can be made simple and safe.

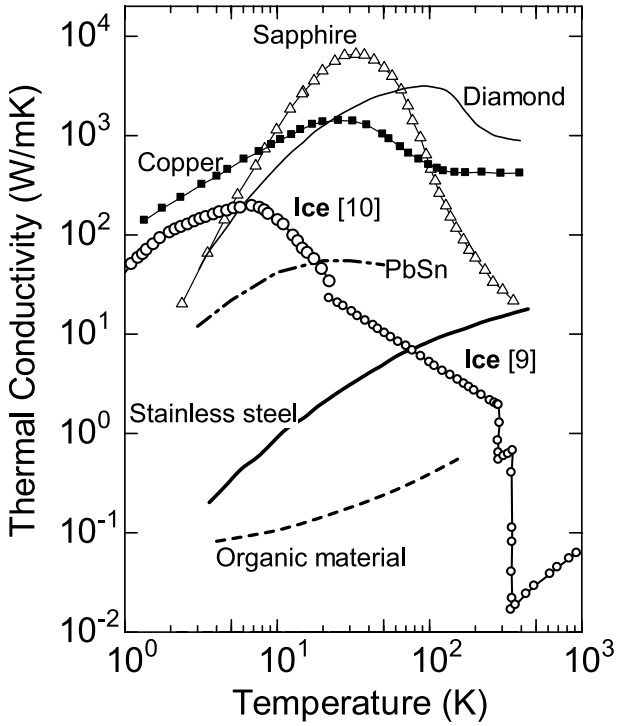

Fig. 3 Thermal conductivities of solid materials [9–11].

In this study, to mitigate the degradation, we employed ice as a molding medium among cable strands. As shown in Fig. 3, the main advantage of ice is its large thermal conductivity [9, 10]. Other advantages of ice include its rigidity at cryogenic temperature, large electric resistance, flexibility, and low viscosity at room temperature [12]. Finally, we successfully mitigated the degradation using ice molding without losing the stability.

2. Experiments

Specifications of a superconducting cable for TRAPSE sample are given in Table 1. A photograph and schematic illustration of the sample without a mandrel are shown in Figs. 4 a) and b), respectively. Figure 4 c) represents the equivalent electric circuit. Figure 4 d) shows a photograph of ice-molded sample B1. A cable was wound three turns around a stainless steel mandrel and heat treated at 700°C for 100 h to form Nb_3Sn superconductor. Plated chromium on the strands was removed from both ends of the cable using hydrochloric acid after the heat treatment. Both ends were soldered together into a praying hands lap-joint configuration. The joint resistance must be as small as possible to induce large currents up to the critical current. The joint resistance was evaluated to be several nΩ. The top single turn in Fig. 4 was compressed between an upper compressing jig and the mandrel itself, which is movable in the vertical direction. In the ice-molded samples, the surface of the compressing jig was coated with fluorinated resin to prevent it from sticking to the mandrel. Three extensometers were installed to measure the deformation of the compressed portion.

Table 1 Specifications of the superconducting cable.

Material		Nb_3Sn
Cu/SC		1.5
Diameter of the strand	[mm]	0.78
Diameter of the cable	[mm]	~5
Cabling pattern		$(2 + 1) \times 3 \times 3$
1st twist pitch	[mm]	30
2nd twist pitch	[mm]	40
3rd twist pitch	[mm]	60
Length of the cable without joint	[m]	0.68
Length of the joint	[m]	0.17
I_c	[A]	104 at 12 T
Samples		
	A	Nb_3Sn cable
	B1and B2	ice-molded Nb_3Sn cables
	B1′	unfrozen B1 cable

A bias magnetic field was applied in the vertical direction in Fig. 4, and the compressed single turn was located at the center of the bias magnetic field. Near the joint, a Hall sensor was attached to measure the circuit current, and a heater was installed to break the induced current.

Larger currents can be induced by increasing the number of turns. However, this results in a large unbalanced electromagnetic force in the axial direction of the mandrel, as the compressed single turn located at the top of the winding must be at the center of the bias coil. This means other turns must be located off-center of the bias magnet. Therefore, to avoid an unbalanced electromagnetic force, we limited the number of turns to three, compromising on the requirement of a large induced current.

The initial diameter of the cable was about 5.0 mm. After the experiment, in which a large mechanical load was applied to the cable in the axial direction of the man-

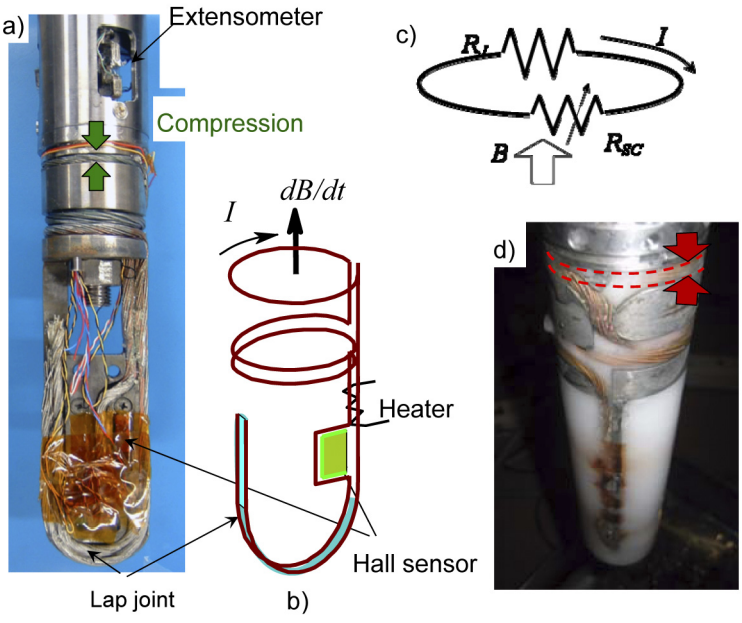

Fig. 4 a) Photograph of TRAPSE sample A, b) schematic illustration of the wound cable, c) equivalent circuit, and d) photograph of the ice-molded sample B1.

drel, the height of the cable reduced to less than 4.0 mm. Therefore, we designed and fabricated an extensometer to measure displacement of more than 1.5 mm. Three of these clip-gauge type extensometers made with TiVAl alloy frames and four strain-gauge bridges were used. The average of the measured values is defined as the deformation of the cable. The load was applied by a geared DC motor and a mechanical jack. Here, 20 kN corresponds to ~29 MPa averaged stress in the projected area of the compressed cable.

The saturation current I_s, which was generated by the induced voltage and regulated by the flux flow voltage in the cable, was measured by the Hall sensor. However, when the electromagnetic force increased, the alignment of the sample became worse, and the Hall sensor detected a component of the bias field. The saturation current was also evaluated from the lap joint voltage $R_J I_s$. The lap joint voltage signal had a good signal-to-noise (S/N) ratio. The magnetic field dependence of the resistance of the soldered joint was found to be negligibly small in our previous study [13].

The circuit equation of the equivalent circuit in Fig. 4 c) is given by Eq. 1.

$$\frac{d\phi}{dt} = L\frac{dI}{dt} + R_J I + R_{SC}(I, B, T, \varepsilon)I \quad (1)$$

The circuit current I is generated by the bias magnetic flux change $d\phi/dt$ [7,8]. The induced voltage $d\phi/dt$ is constant during the monotonous ramp up of the magnetic field, and is balanced by the sum of the inductive voltage of the closed circuit $L(dI/dt)$, joint voltage $R_J I$, and superconducting cable voltage $R_{SC}I$. Here, R_{SC} is the electric resistance of the superconducting cable in the flux flow state. Since R_{SC} is given by the V–I characteristics of the cable, it is affected by the current I, magnetic field B, temperature T, and mechanical strain ε.

In a critical current measurement, the electric field criterion is constant, e.g., 1 μV/cm. In other word, the critical current is the saturation current measured using a constant voltage power supply generating an electric field of 1 μV/cm. In our experiment, the electric field is determined by subtracting $R_J I$ from the induced voltage, which is less than ~3 μV/cm. This is obtained assuming the induced voltage of 34 μV at the ramp rate (dI_{bias}/dt) of 4 A/min and an effective compressed cable length of 0.1 m. Note that the electric field in the cable is not constant as the joint voltage $R_J I$ changes with saturation current I_s, whereas $d\phi/dt$ is constant. Therefore, we call it saturation current in our experiment. However, I_s and I_c for low T_c superconductors (LTS) with relatively large n index are almost identical at high magnetic fields, as reported in [6].

The test was performed in liquid helium using the 18 T superconducting magnet at Tohoku University. The maximum ramp rate of the bias magnetic field is 0.58 T/min, which corresponds to dI_{bias}/dt = 7 A/min. After the mechanical load reached the desired value, the gear was stopped, and the bias magnetic field was ramped up and down. Through this procedure, the magnetic field dependence of I_s was continuously monitored.

3. Results

Figure 5 shows saturation currents with various loads. When the bias magnetic field is increased, a positive current flows in the closed loop to shield the external magnetic field. In contrast, while the bias magnetic field is decreased, a negative current traps the magnetic field in the loop. By applying a load, the saturation current decreases. For example, it degraded by more than 50% from its original value with a 20 kN load [6].

Results of the saturation current measurement for ice-molded sample B1 are shown in Fig. 6 a). No degradation due to compressive load was observed. In contrast, as shown in Fig. 6 b), for sample B1′, which is obtained after unfreezing the ice in sample B1, degradation similar to the original cable sample, i.e., sample A, was observed.

In Fig. 7, degradations in various samples are summarized. It was found that the medium between the strands is effective in mitigating the degradation for up to 27 kN compressive load. Saturation currents do not recover when the cable is unloaded [6]. This means that the superconducting material might be mechanically damaged by the transverse load.

Figure 8 shows load–displacement curves during the test. Here, the horizontal spike signals should be ignored because these are assumed to be inductive noises during the energization of the bias magnet. Ice-molded sample B has a large Young's modulus similar to heavily deformed sample A. The curve for 1000 load–unload cycles was obtained and plotted only for sample A. Due to ice molding, Young's modulus is increased. Ice between the strands is

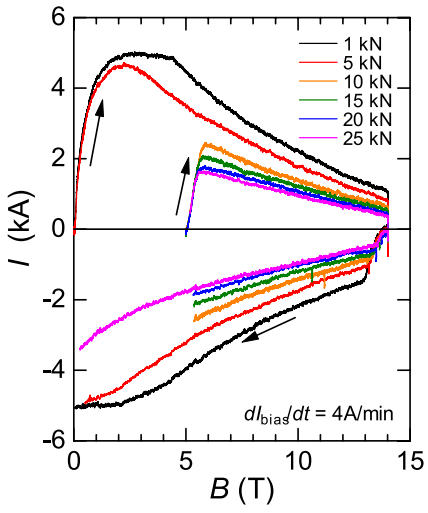

Fig. 5 Magnetic field dependences of saturation current in sample A without ice molding for various transverse loads [6].

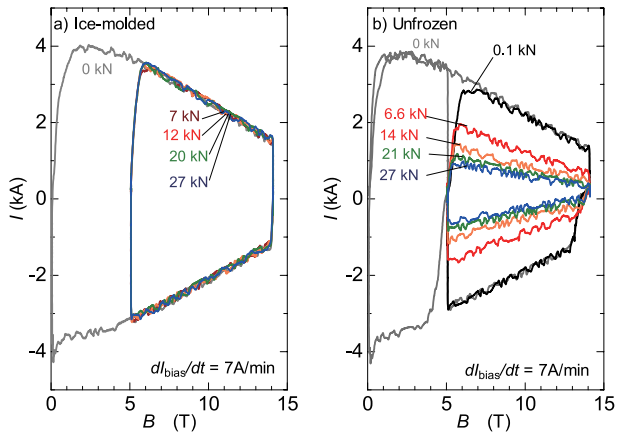

Fig. 6 Magnetic field dependences of saturation current. a) Ice-molded sample B1 and b) unfrozen sample B1′ for various transverse loads.

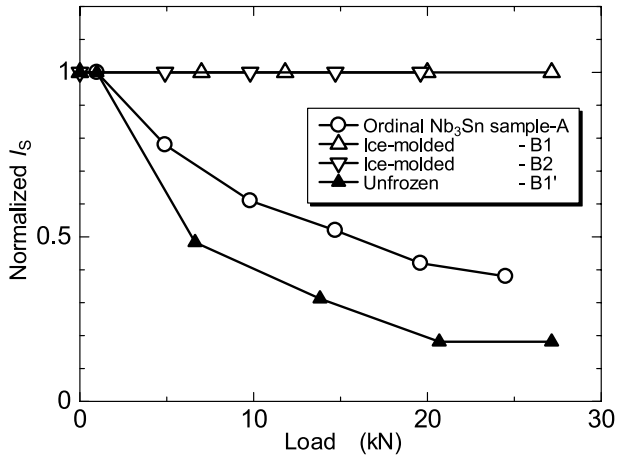

Fig. 7 Degradation of saturation currents due to mechanical loads in a 12 T magnetic field.

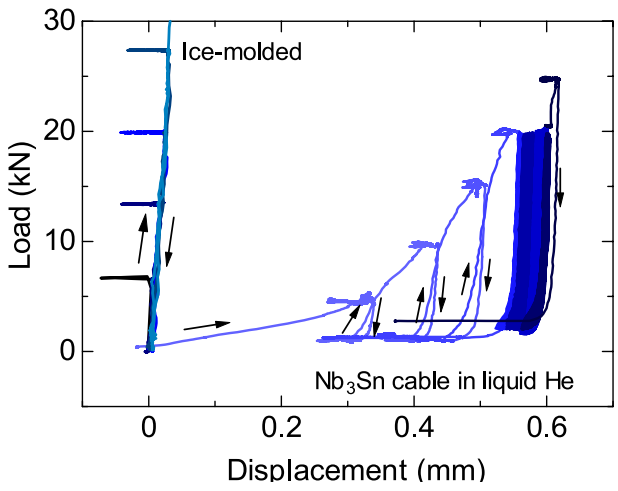

Fig. 8 Load–displacement curves during the tests. Averaged values of three sensors are plotted for samples A and B1.

stiff enough to mitigate the deformation of the cable.

4. Discussion

The degradation of the saturation current in the Nb3Sn cable was around 50% at an average stress of ~20 MPa, i.e., 13.8 N in load. This is larger than the reported experimental results of actual conductors in coils or short samples [4]. One reason is as follows: In an actual conductor, the Lorentz force is a body force as shown in Fig. 2. Hence, one strand, which is twisted by multiple stage twisting, experiences various magnitudes of stress along its length. In contrast, in our sample, the force is external. Therefore, the stress distributions along individual strands are relatively flat, and all strands were compressed equally. Consequently, our study tends to overestimate the degradation due to transverse loading.

To mitigate this degradation in critical current, we investigated the possibility of molding the void between strands with ice. No quenching was observed in Fig. 6 b). Due to the large thermal conductivity of ice, it is possible to mold the superconducting cable without losing its stability. In addition to its rigidity and thermal conductivity, ice has several advantages, e.g., small viscosity and infinite pot life at room temperature [12].

In any case, further innovations will be required for a superconducting magnet in future systems as explained in Fig. 1. The experimental setup proposed in this study is useful for investigating new configurations and materials for future conductors.

5. Conclusion

We developed a saturation current test facility that employs the induced current technique. Our method is a simple critical current measurement technique for a superconducting cable.

For an average stress of 30 MPa, the saturation current degraded to less than half of the original value. In contrast, reinforcement by ice molding perfectly mitigates the degradation. Because of the large thermal conductivity of ice, the stability of the superconducting cable can be guaranteed and no quenching occurred while maintaining the electric field.

Acknowledgments

Part of this work was supported by a Grant-in-Aid for Scientific Research (17656098) and Fusion Engineering Research Center program at NIFS (NIFS06UCFF005). This work was performed at the High Field Laboratory for Superconducting Materials, Institute for Materials Research, Tohoku University.

[1] ITER Design Description Document (DDD), 11, Magnet (N 11 DDD 177 04-05-12 W 0.2) (2004).
[2] A. Nishimura *et al.*, J. Plasma Fusion Res. **83**, 30 (2007).
[3] N. Mitchell, Cryogenics **43**, 255 (2003).

[4] A. Ulbricht, J.L. Duchateau, W.H. Fietz, D. Ciazynski, H. Fillunger, S. Fink *et al.*, Fusion Eng. Des. **73**, 189 (2005).
[5] K. Seo, Y. Hishinuma, A. Nishimura, G. Nishijima, K. Watanabe, K. Nakamura, T. Takao and K. Katagiri, Fusion Eng. Des. **81**, 2497 (2006).
[6] K. Seo, A. Nishimura, Y. Hishinuma, K. Nakamura, T. Takao, G. Nishijima, K. Watanabe and K. Katagiri, IEEE Trans. Applied. Supercond. **17**, 1390 (2007).
[7] P. Fabbricatore, R. Musenich, R. Parodi, D. Truffelli and G. Zappavigna, IEEE Trans. Magn. **27**, 1818 (1991).
[8] G.B.J. Mulder, H.H.J. Ten Kate, A. Nijhuis and L.J.M. Van de Klundert, IEEE Trans. Magn. **27**, 2190 (1991).
[9] S. Iida, *New edition - Table of physical constant* (Asakura Publishing Co., Ltd., 1978) p.123 [*in Japanese*].
[10] J. Klinger and G. Rochas, J. Phys. Chem. B **87**, 4155 (1983).
[11] T. Shigi *et al.*, *Cryogenic Engineering Handbook* (Uchida Rokakuho Publishing Co., Ltd., 1982) p.582 [*in Japanese*].
[12] V.F. Petrenko and R.W. Whitworth, *The Physics of Ice* (Oxford University Press, 1999) ISBN 0-19-851895-1.
[13] K. Seo, S. Nishijima, K. Katagiri and T. Okada, IEEE Trans. Mag. **27**, 1877 (1991).